communications earth & environment

ARTICLE

https://doi.org/10.1038/s43247-022-00569-5 OPEN

Global patterns of sea surface climate connectivity for marine species

Panagiotis Petsas [1]✉, Aggeliki Doxa[1,2], Vasiliki Almpanidou [1] & Antonios D. Mazaris[1]

A potential strategy for marine species to cope with warming oceans is to track areas with optimal thermal conditions and shift their spatial distributions. However, the ability of species to successfully reach these areas in the future depends on the length of the paths and their exposure to extreme climatic conditions. Here, we use model predictions of sea surface temperature changes to explore climate connectivity and potential trajectories of marine species to reach their optimal surface thermal analogs by the end of the century. We find that longer trajectories may be required for marine species of the northern than the southern oceans and that the former may be more exposed to extreme conditions than the latter. At key biodiversity hotspots, most future surface thermal analogs may be located in very remote areas, posing a significant challenge for local species to reach them. The new marine connectivity approach presented here could be used to inform future conservation policies.

[1] Department of Ecology, School of Biology, Aristotle University of Thessaloniki, Thessaloniki, Greece. [2] Institute of Applied and Computational Mathematics, Foundation for Research and Technology-Hellas (FORTH), Heraklion, Crete, Greece. ✉email: pnpetsas@bio.auth.gr

Climate driven redistribution of marine biodiversity is expected to trigger the reorganization of ecosystems, altering the functionality and services provided[1,2]. Certain factors are forcing species to shift their ranges to maintain favorable environmental conditions[3], including the accelerating rate of ocean warming[4], novel climates (i.e., new climatic conditions that were not found in the past[5]), and increased occurrence of marine heatwaves[6,7]. For instance, the distributions of two thirds of fish species in the North Sea shifted by mean latitude or depth between 1977 and 2001[8]. Similarly, multiple fish species in the South Sea of Australia have exhibited major climate-related shifts in distribution[9]. A poleward shift at the cooler edges appears to be a key climate-driven response of organisms tracking the shifting isotherms, with some exceptions[10–12].

However, following a shifting climate is not feasible for all species. The limited ability of some species to disperse at the rates of climate change, and the loss of suitable climate, could result in inefficient shift responses. Hence, it is critical to quantify climate connectivity[13] for trajectories between sites that have specific climatic conditions and sites that will have these conditions in the future (hereafter, thermal analogs), facilitating species persistence in a changing planet. Former attempts to project climate trajectories that describe the shift of climate isotherms through time were based on delineating single paths that minimize the distance between thermal analogs[14,15]. However, these methods overlook the actual exposure of species to climatic differences along the routes, which could hinder species movement[16]. Consequently, studies have started accounting for climatic exposure between thermal analogs by delineating paths that minimize exposure to dissimilar climates over delineated periods[16,17]. Yet, these studies only use climatic data for two distinct periods, reflecting present and future conditions, as they interpolate the intermediary climate with a linear function. While this approach accounts for temperature increments, it fails to incorporate the potential impact of extreme climatic events during the focal period. Therefore, generated outputs are likely to highlight climatic trajectories that are not actually suitable for minimizing climate exposure.

Here, we assess global connectivity of the marine surface climate by spatially delineating climate trajectories between the current thermal conditions and their future surface thermal analogs (hereafter mentioned as "thermal analogs"). We used sea surface temperature data from historical and future projections, based on the moderate Shared Socioeconomic Pathway (SSP) 2–4.5 and on the more severe SSP 5–8.5 scenario. The temporal interval covered a total of 150 years, from 1951 to 2100. We also investigated mid-century thermal analogs (from 1951 to 2050). To account for different dimensions of sea surface climatic conditions, we defined unique climates, and identified thermal analogs based on a combination of bioclimatic variables. To delineate trajectories that connect thermal analogs, while avoiding exposure to non-analog conditions, we generated cost surfaces for all unique climates, indicating climatic dissimilarity. We created cost surfaces for each consecutive five-year period from 1951 to 2100 (30 in total), with the minimum cost per pixel over all periods being used to produce the final cost surface. To highlight important areas that could facilitate the movement of organisms between thermal analogs and areas with low climate velocity (i.e., distance to closest thermal analog), we applied four metrics derived from circuit theory[18] and least-cost path analysis[19]. The applied metrics incorporate a cost scheme for the seascape, allowing the climatic exposure of trajectories between thermal analogs to be accounted for. To illustrate possible implications for management, we evaluated the climate connectivity patterns among surface ocean pixels located within the Major Fishing Areas (MFAs) and further investigated the location of future thermal analogs for six key marine biodiversity hotspots, as delineated by Ramirez et al. (2017)[20]. Our study indicates that marine species in the Northern Hemisphere will be forced to travel longer distances to reach their future thermal analogs than those in the Southern Hemisphere, with greater exposure to dissimilar climates. Moreover, we found that thermal analogs for key biodiversity hotspots may be located in distant areas in the future, raising concerns on the ability of local species to reach them.

Results and discussion

Our analysis revealed similar patterns of future sea surface connectivity when using both the moderate (SSP 2–4.5) and severe (SSP 5–8.5) climatic scenarios. These two scenarios generated consistent outputs for both short-term (2050) and long-term (2100) future analogs. Strong significant associations were detected for all pair-wise comparisons of the connectivity metrics under both scenarios. Therefore, we only presented the outputs generated under SSP 5–8.5 for the long-term future analogs here (See Supplementary Methods S1, Tables S3–S7, Figs. S6–S11 for the other output).

Sea surface thermal analogs. Our study showed that more than one fourth (27%) of surface ocean pixels had no thermal analog, indicating that their unique climatic conditions would be lost by 2100 (Fig. 1). Most of these pixels were found in northern oceans, which are affected by high warming rates[21,22]. The northern oceans mostly hosted thermal analogous conditions to those currently observed in more southern areas. This finding was consistent with existing studies, indicating that species will have to move northward to meet their preferred climatic conditions[11,12]. Almost one fifth (19%) of pixels were projected to experience novel climates in the future; consequently, these pixels could not host climatic conditions of the recent past. These pixels primarily occurred in the tropics, likely reflecting the extreme climatic events of this zone[23]. About 4% of ocean pixels had no thermal analog, nor would they be thermal analog for other climates in the future. Most of these pixels were located in the tropics (equatorial Pacific Ocean).

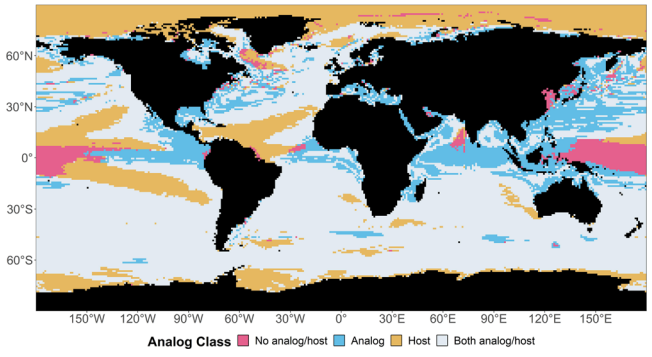

Fig. 1 Global marine map showing pixel classification based on thermal analogous conditions. Pixels are grouped in four classes: (i) will not have a thermal analog and will not host past thermal conditions in the future (red); (ii) will have a thermal analog, but will not host past thermal conditions in the future (blue); (iii) will not have a thermal analog, but will host past thermal conditions in the future (orange); and (iv) will have a thermal analog and will host past thermal conditions in the future (white). Black pixels represent land mass, water masses that are blocked by land mass, and pixels with no climatic data.

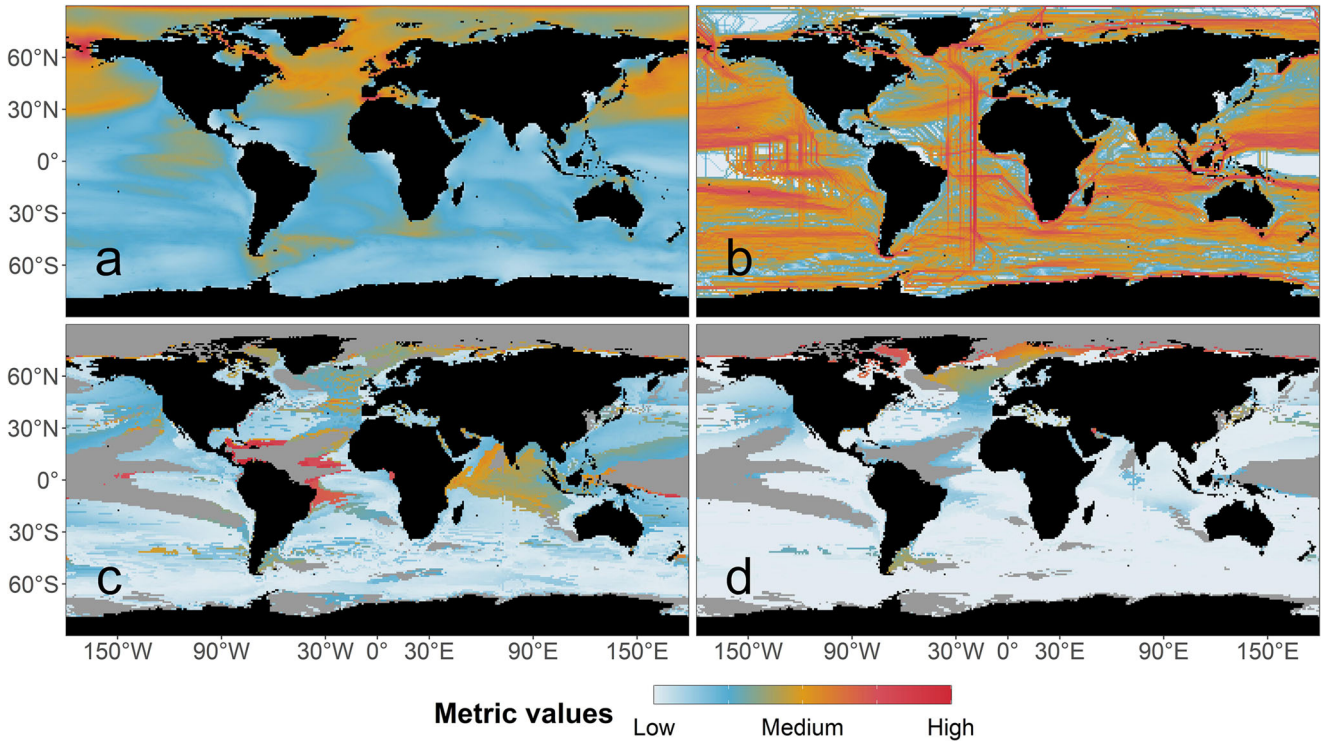

Fig. 2 Global map of the marine environment showing pixel prioritization based on four connectivity metrics. The metrics displayed are current flow **a**, path density **b**, minimum exposure distance, **c** and minimum cumulative exposure **d**. Pixels were evaluated based on how they facilitated movement between thermal analogs **a**, **b**, the length of the trajectory used to reach their thermal analogs **c**, and exposure to dissimilar climates through that trajectory **d**. Metric values ranged from low (white) to high (red). Values for **a** and **b** were log-transformed to aid interpretation. Pixels with no thermal analogs in **c** and **d** are shown in grey. Pixels with no climatic data, land masses, and water masses that are blocked by land masses are shown in black.

Oceanic areas that promote climate connectivity. As the global climate becomes warmer, future analogs of current local climatic conditions may be found in distant areas[14,16]. For organisms to avoid passing through areas of highly dissimilar climatic conditions, trajectories between thermal analogs mostly pass through specific sites that minimize climatic exposure. Across the seascape, pixels that could facilitate movement between thermal analogs were found to be spatially aggregated, covering extensive marine areas; however, their extent and distribution varied among oceans and latitudes (Fig. 2a). These areas, which could contribute to climate connectivity under projected shifts of ocean climate, were identified using current flow at each ocean pixel[18]. This metric quantifies the probability that a trajectory between thermal analogs passes through a given pixel. Current flow was projected to be higher in northern areas ($r_s = 0.70, p < 0.01$, Fig. 3a). Overall, oceans in the Northern Hemisphere (i.e., Arctic, north Pacific and north Atlantic oceans) had higher current values, indicating that movement between analogs would become more intense in these oceans compared to oceans in the Southern Hemisphere ($H = 19621, df = 6, p < 0.01$; Supplementary Fig. S1). This phenomenon might be related to the higher warming rate of north[21,22]. Furthermore, extensive land mass in the north constrained the trajectories between thermal analogs, eliminating potential routes. For instance, the highest metric values were found in areas located between North America and Asia (such as the Bering Sea), at Gibraltar (which connects the Atlantic Ocean and the Mediterranean Sea), and at the Baltic Sea in Scandinavia. These areas are formed of narrow passages, where limited alternative routes exist.

Multiple sites near the equator had high path density, with this metric quantifying the number of optimal routes that pass over a pixel[17] (Fig. 2b). Path density had no latitudinal pattern ($r_s = -0.08$, $p < 0.01$) and was weakly correlated with current flow ($r_s = 0.17, p < 0.01$). As path density is based on the optimal routes between thermal analogs, it could be a more representative metric for assessing connectivity potential for highly migratory species, while current flow accounts for multiple pathways, and could be more suitable for species with limited dispersal capacity[18]. Many notable differences between the two metrics were observed in the oceans (Supplementary Figs. S1–2). For example, multiple sites in the Indian Ocean had high path densities but relatively low current flow values. Still, certain marine regions (e.g., North Atlantic Ocean) and areas with narrow passages (e.g., Bering Sea, Gibraltar) were identified as important by both metrics. In addition, multiple sites in the equatorial Pacific Ocean facilitated little to no movement between thermal analogs for both metrics, mirroring evidence on high warming rates in this basin[24] that will likely impede species dispersal.

Climatic velocity. At the tropical and subtropical regions of the Western Atlantic Ocean, many pixels had high velocity but relatively low climatic exposure (Fig. 2c, d). Thus, while these sites had thermal analogs in distant areas, their trajectories would pass over sites with conditions close to optimal thermal ranges. The topographical barriers in this region were limited to the land masses of South and Central America, providing multiple pathways towards thermal analogs. Yet, for many tropical regions across the planet, the rate and magnitude of warming could generate novel climates[25,26], potentially eliminating the connectivity process. There is increasing evidence of widespread declines in marine tropical biodiversity[27–29]. Similarly, future climate, projections have revealed high rates of loss of tropical species[30,31].

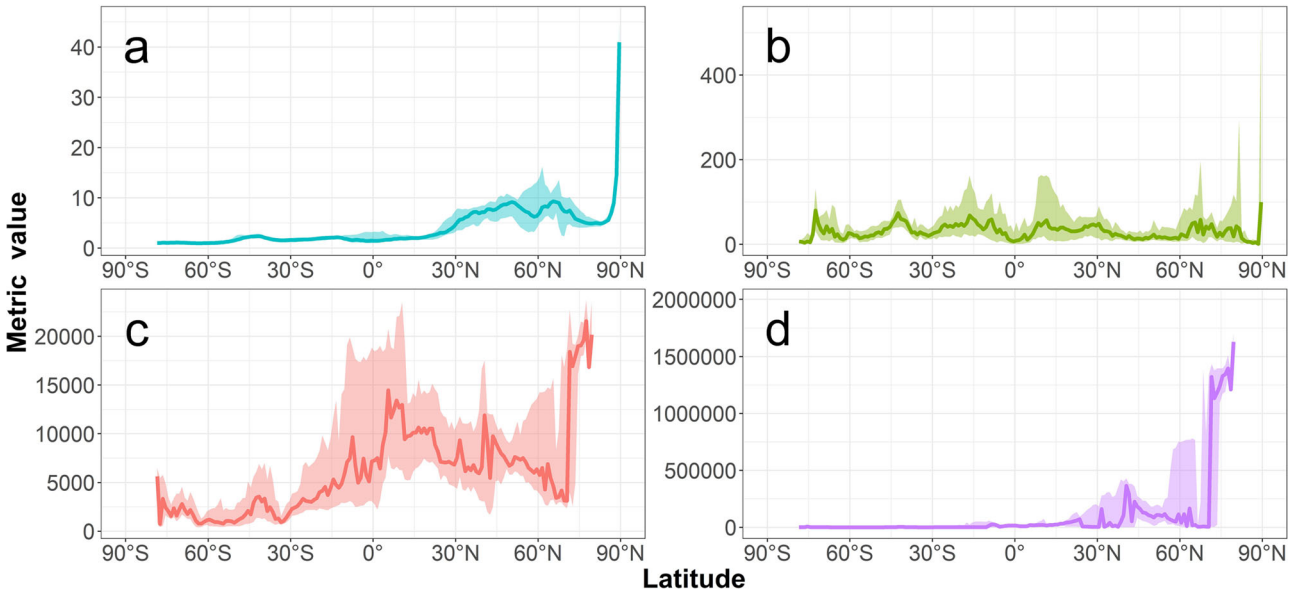

Fig. 3 Median connectivity metric value across a latitudinal gradient. The median value for current flow **a**, path density **b**, minimum exposure distance **c**, and minimum cumulative exposure **d** was calculated for 1° moving windows (solid line). The shaded area corresponds to 25% and 75% quantiles of the metric values per latitudinal point.

The physical barriers created by the land masses in the northern oceans of the planet, along with the higher warming rate in these areas[21,22,32,33], resulted in a latitudinal pattern in climatic velocity ($r_s = 0.59$, $p < 0.01$) and climatic exposure ($r_s = 0.63$, $p < 0.01$) (Fig. 2c, d). The few pixels in the Arctic Ocean that had thermal analogs required longer ($H = 6105.3, df = 6, p < 0.01$, Supplementary Fig. S3) and more exposed transitions ($H = 7858.5, df = 6, p < 0.01$, Supplementary Fig. S4) compared to the other oceans. Major changes to community composition in the Northern Hemisphere are projected in the future[34–36], because the region will be exposed to high warming rate[37]. While there are northern sites with thermal analogs, some species are likely to be further challenged by lower climatic connectivity. For instance, while species in North and Norwegian Seas track analogous climatic conditions quickly, this might not be the case for species in the Barents Sea[12], which is projected to be exposed to high warming[37]. In contrast, pixels in the Southern Hemisphere have lower velocity and climatic exposure values, indicative of less distant thermal analogs, passing through similar climates during the transition. Approximately 14% of pixels with thermal analogs had a climatic exposure value of zero, with most occurring in the Southern Hemisphere (Fig. 2d). Still, the tolerance of different marine organisms to warming and changes to productivity, along with sea ice characteristics and seasonal dynamics, would further challenge their ability to track their suitable climatic conditions[38]. In particular, species of great ecological significance in the Southern Hemisphere, such as Antarctic krill, are highly vulnerable to climate change, which will drive changes to their distributions[39].

Connectivity between major fishing areas (MFAs). Large spatial variations were prevalent in connectivity patterns among MFAs, as defined based on the proportion of the surface expected to have or become (i.e. host) a thermal analog by 2100. MFAs close to equator were projected to relatively have more analogs, while southern hemisphere MFAs had in general higher proportions of areas with future thermal analogs than northern ones (Fig. 4). Moreover, two southern hemisphere MFAs, the Southeast Pacific Ocean and the Eastern Indian Ocean (i.e., No 87 and 57 in

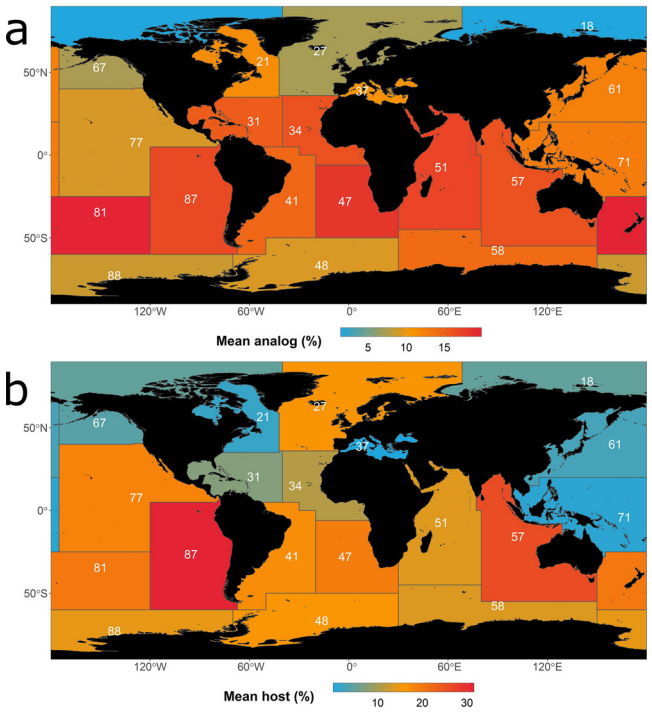

Fig. 4 Connectivity status on Major Fishing Areas (MFAs) from Food and Agriculture Organization (FAO). Each MFA is presented by its unique identification number (label). Connectivity metrics represent the mean percentage of pixels that will have an analog in the other MFAs in the future **a** and the mean percentage of pixels that will host analogs from other MFAs in the future **b**.

Fig. 4b) hosted more thermal analogs (31.5 and 26% of total surface respectively) than other MFAs. Nonetheless, for all MFAs, future thermal analogs were mostly observed in long-distance areas. For example, current local climate conditions of sites in the Northeast Pacific Ocean had their future analogs in the Northeast Atlantic Ocean (Supplementary Fig. S12). These findings on sea

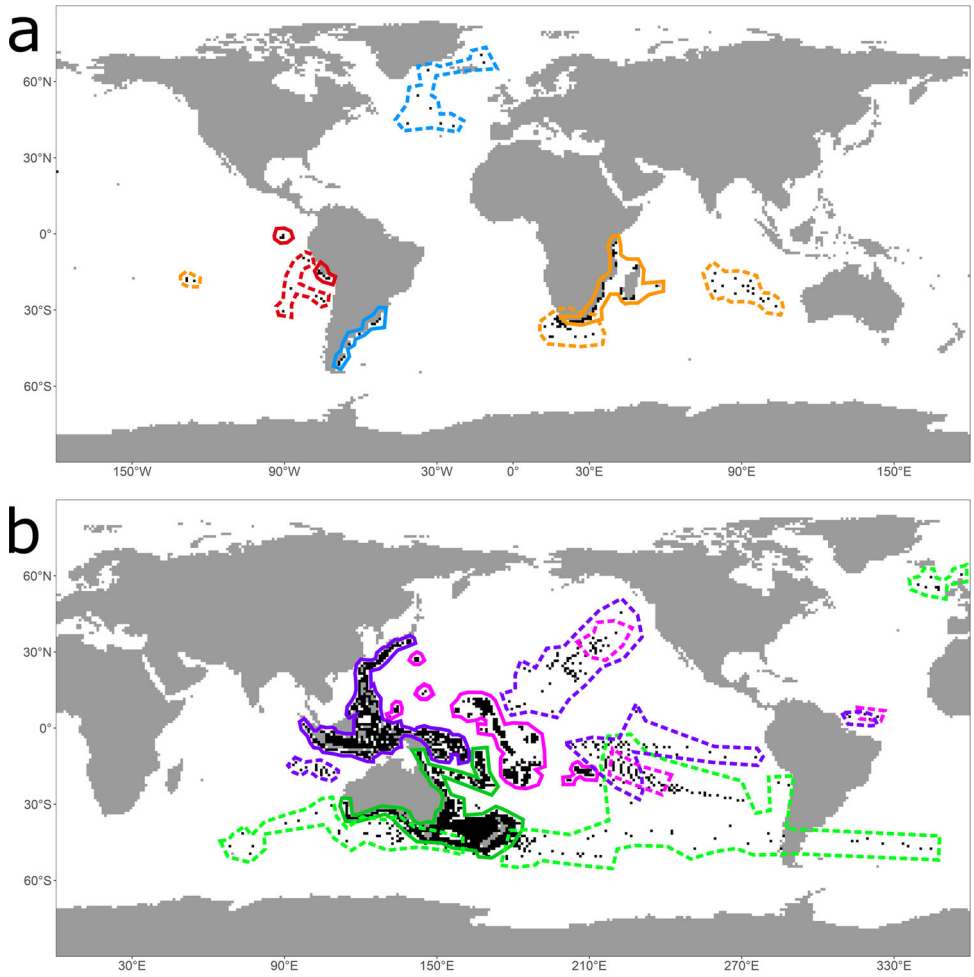

Fig. 5 Key biodiversity hotspots and their thermal analogs. Black pixels are either part of a hotspot or future analogs for a hotspot pixel. Solid lines enclose the hotspot pixels in the present, while the dashed lines enclose the hotspot's future analogs. Each hotspot, along with its analogs is presented with a different color. In **a** the three hotspots identified in South America and Africa. In **b**, the three hotspots in East Asia and Oceania, with East-degrees projection to aid interpretation.

surface climate connectivity patterns underline the fact that, for many species, possible range shifts would not be efficient enough to track and reach thermal analogous areas.

Biodiversity hotspots and their future thermal analogous sites. The analyses on key marine biodiversity areas further supported these concerns, as future thermal analogs were mostly found in thousands of kilometers apart from the current biodiversity hotspots (Fig. 5). These long distances exceed dispersal capacities of most marine species[40]. Furthermore, the fact that the current hotspots are mostly found close to coastal areas, while their future analogs are almost always located in the open sea, indicate that future thermal analogs may not serve as future habitat analogs for the species, highlighting the potential risk for the perseveration of marine biodiversity within the following decades.

Future enhancements of climate connectivity methodological framework. Methodological approaches permitting the efficient modeling of climate connectivity, while also considering narrow time-lag intervals when investigating future thermal analogs, are lacking[17]. The methodology presented here could serve as a step towards addressing this challenge, providing the means to account for climate-driven species displacements and potential movement pathways, in addition to short-term thermal barriers, which might limit the ability of organisms to migrate to maintain their thermal niche. Here, we used data from current and future projections of ocean surface temperatures, based on the CMIP6 models. To our knowledge, these are the most accurate climate projections currently available at the global scale, with slight improvements over the CMIP5 models[41–44]. Nevertheless, these models are subjected to biases; for example predictions on El-Nino warming pattern in the equatorial Pacific ocean, indicate faster warming in the east than in the west[45,46]. These biases could potentially lead to an underestimation on connectivity status, as multiple pixels in this region were projected to fail hosting climatic conditions of the recent past (Fig. 1). Similar biases are present for modeled historical data, such for the case of equatorial pacific cold tongue[47], which could also have an effect on the proper identification of future thermal analog pixels. However, the alternative use of historical observed data would not be suitable in our case, as their production is based on a number of assumptions, leading to biases that differ from the ones in CMIP models. On the contrary, by using the same global circulation models (i.e. CMIP6) for both present and future data, it is guaranteed that these biases are propagated equally across the entire time period studied[48]. Considering that each specific CMIP model has distinct assumptions, sea surface connectivity patterns could be affected by the climatic model selected as sea surface input. To overcome this limitation, we selected an ensemble

model that provides mean temperature values from multiple models instead of a single one, mitigating the potential over- or under-estimation of sea surface temperature from specific models.

Yet, although the results of our analysis are valid in terms of surface thermal habitat, other factors such as ocean structure, currents, oxygen concentration, salinity and prey availability are also important[49,50]. Additional environmental information could facilitate a more comprehensive approach that accounts for species specific preferences. More importantly, while sea surface temperature is traditionally used to project climate-related patterns at different spatial and temporal scales[51,52], and to explore a range of potential responses of marine organisms[3,12], the marine realm is inherently three-dimensional. Assuring vertical coherence of marine ecosystems against climate change impacts could prevent risking the disruption of trophic interactions and reduce exposure to novel climates[48,53]. Within this framework, information on species observations, potential responses, and climate redistribution patterns across the three dimensions should be considered[54,55] to move towards future climate-smart conservation planning approaches and networks[56]. The methodological framework introduced in this paper could be applied at various spatial scales and different depths, encouraging future studies to investigate multi-variable and multi-dimensional connectivity patterns.

Conclusions

To support conservation planning, several tools have been developed to project potential climate-driven shifts of species distribution. For instance, ecological niche models[57], metrics of the velocity of isotherm shifts[15,58], and spatial patterns of future thermal analogs[16,59], offer projections of future redistribution of biodiversity. Many such spatial trajectories are now available and are being used to assess conservation efficiency and policy recommendations[54,60]. Yet, our results demonstrate that delineating potential isotherm shifts based on distinct time slots of climate alone (i.e., current and projected climatic niche, climate change velocity over distinct periods, thermal analogs) largely overlook the inherent dynamics of seascape climate. For example, while the increased warming rate of the northern seas might force local species to exhibit certain movements to capture favorable climatic conditions, our findings on distant analogs, connected by paths that are exposed to extreme climate, lead us to question the ability of the species to perform such movements successfully. The framework presented here provides a foundation on which to explore the potential of the projected climate driven distribution shifts of marine organisms, under the dimension of climate connectivity. We, thus, call for future research that incorporates the methods and outputs presented here towards providing a more comprehensive view of future range shifts in the marine environment.

Methods

Climate data. To assess the climate of the global ocean, we combined daily data of historical and future temperature projections from 11 ocean surface temperature models (Table S1) from Coupled Model Intercomparison Project phase 6 (CMIP6)[61]. Initially, for each model, we used the daily data to calculate the minimum and maximum monthly data per year. To obtain a more comprehensive estimate of climatic conditions for time intervals larger than a single year, we regrouped the yearly datasets into 30 five-year periods (hereafter, called periods). Then, we calculated the mean minimum and maximum monthly data for each five-year period. To obtain an ensemble sea surface temperature model, we combined all 11 models by extracting the mean minimum and maximum monthly data per period. This process resulted in 24 climatic layers per period (i.e., 12 for minimum and maximum monthly data, respectively). The data provided by the 11 ocean surface temperature models were available on native grids, so they were transformed to a regular grid using the "akima" package in R. Then, the data were interpolated to a common grid of 1° × 1° resolution, using the "resample" function in R, under bilinear interpolation, which is used for continuous variables.

The time period studied here covered 150 years, extending from 1951 to 2100. Future projections are based on the Shared Socioeconomic Pathways (SSP) 5–8.5 and 2–4.5[62]. Climatic connectivity outputs, generated under the two SPPs, were then compared (see Supplementary Methods S1, Tables S3–S7, Figs. S6–S11 for details on this sensitivity analysis). To explore the sensitivity of our outputs to the climate scenarios used, we compared the connectivity patterns between thermal analogous sites over short-term (2050), rather than long-term future climatic conditions (2100), under both SSP 2–4.5 and 5–8.5 scenarios. We also examined whether the length of the periods affected our results, by repeating the analysis with 10-year periods instead of 5-year periods.

Bioclimatic variables. For each period, we calculated nine bioclimatic variables that express seasonal trends and extreme temperature values (Table S2). These variables were calculated based on the minimum and maximum monthly temperature data obtained by our ensemble temperature model (see Climate data section). To reduce the number of variables, while maintaining the information provided, we performed a principal component analysis. Our variables fulfilled the requirements for this analysis, as they consisted of a large number of records (i.e., 42864 pixels), were significantly correlated under the Pearson correlation coefficient ($p < 0.05$), with mostly high correlation values, indicating linearity, and there were few outliers. We reduced the bioclimatic variables to two principal components (hereafter, *PC*1 and *PC*2, Supplementary Fig. S5), which explained 93.3% of the variance in the original variables. Following this process, we generated 60 climate layers (i.e., two principal components for each period).

Defining climates. The values of the two principal components were scaled based on the minimum and maximum values of the first period (i.e., 1951–1955), using the following formula[17]:

$$PC_i' = 1 + 99 * \frac{PC_i - min\{PC_1\}}{max\{PC_1\} - min\{PC_1\}} \quad (1)$$

where PC_i denotes a principal component for period i. Using this formula, the principal component values in the first period were scaled in the range of [1, 100], while those for other periods could fall out of this range, indicative of novel climates. To classify the principal component values, we created two sets of bins, one per component. The bin centers were integer values, of ± 0.5 width, covering all *PC* scaled values. There were 116 bins for *PC*1 and 104 bins for *PC*2, resulting in 12064 possible combinations. These bin combinations were used to define climate. We identified 2780 different climates in the first period.

Thermal analogs and their connections. A pixel was considered to have a thermal analog if its thermal conditions in the first period (i.e., 1951–1955) was observed in the last period (i.e., period 30; 2096–2100), either on the same pixel or a different pixel. Following this process, each pixel was classified into one of four classes: (i) will have a thermal analog and will host past thermal conditions in the future; (ii) will have a thermal analog but will not host past thermal conditions in the future; (iii) will not have a thermal analog but will host past thermal conditions in the future; and (iv) will not have a thermal analog and will not host past thermal conditions in the future.

To quantify the exposure of trajectories between thermal analogs to dissimilar climates, we constructed cost surfaces. Following Carroll et al.[17], cost surfaces indicate the climatic dissimilarity of the seascape for a given climate (i.e., difference in *PC*1 and *PC*2 values). For each unique climate, we constructed 30 cost surfaces (one per period). The total cost for pixel k is:

$$cost(k) = 1 + p * \left|PC1 - PC1(k)\right| + p * |PC2 - PC2(k)| \quad (2)$$

where *PC*1 and *PC*2 denote the *PC* values of the specific climate; $PC1(k)$ and $PC2(k)$ denote the *PC* values of pixel k; and p is the dissimilarity penalty. In our case, $p = 2$[16,17], indicating that a unit of difference between the scaled *PC* values increases the cost by 2. The sensitivity of our results to cost penalty was also examined, by using alternative cost values, which did not alter the observed patterns in connectivity (see Supplementary Table S6). The final climate cost surface, which integrated all periods, was derived as the minimum cost per pixel from all periods.

Connectivity metrics. To quantify climate connectivity between thermal analogous ocean surface pixels, we used four metrics. These metrics used the cost surfaces to quantify the extent to which the seascape impedes connectivity between pixels. The first two metrics were current flow[18] and path density[17] and were used to evaluate pixels based on the extent to which they facilitates movement between thermal analogs. Current flow is a metric derived from circuit theory[18]. It models the displacement of an individual that moves randomly on a raster mosaic between two thermal analogs. The movement from one pixel towards its considered future analog is based on a cost surface, with low-cost pixels having a higher probability to be selected as the next movement step. The final output is a current flow map, indicating the pixel-wise probability that the trajectory between the thermal analogs passes through it[18]. We used this metric as an ensemble for all trajectories, quantifying the overall pixel-wise probability that a trajectory between any pair of thermal analogs passes through a given pixel. Path density[17] is based on least-cost

path algorithm[19]. Based on the cost surface, this algorithm extracts the trajectory between two thermal analogs with the minimum cumulative cost. This trajectory has two attributes, its length and its cumulative cost[19]. Path density measures the number of these trajectories that cross a pixel. Therefore, for a given pixel, the key difference between the two metrics is that for current flow estimation, we assume that an individual organism moves randomly, based on climatic dissimilarity, whereas for path density calculations, we only consider the trajectories that minimize climatic exposure (i.e., least-cost paths)[19]. Path density accounts for specific trajectories along which organisms move with prior knowledge of the climate, and thus traverse through the seascape, while minimizing climatic exposure. Current flow, given the limited knowledge of the seascape, is used to quantify movement towards all thermal analog pixels. Conversely, path density only accounts for the trajectories of a pixel to its thermal analog with the minimum cumulative cost (i.e., the minimum climatic exposure).

The other two metrics used here were minimum exposure distance (MED)[16] and minimum cumulative exposure (MCE)[16]. These metrics indicate the effort required for an individual (i.e., species) to reach the thermal analog. These two metrics were only available for pixels with thermal analogs. To calculate these metrics for a given pixel, we first extracted the trajectory to its thermal analog that minimizes climatic exposure, by using the least-cost path algorithm[19]. MED quantified climatic velocity, which is defined as the length attribute of the extracted trajectory. MCE is a complementary metric that is used to quantify the exposure to dissimilar climates during this transition, being equal to the difference between the trajectory's cumulative cost and its length[16]. When a pixel has multiple thermal analogs, the values maintained are those obtained from the trajectory with the lowest climatic exposure.

We also used these metrics to examine the connectivity status at the ocean level. We extracted ocean boundaries from the International Hydrographic Organization (IHO) Sea Areas v3 (www.marineregions.com). For all seven ocean basins (i.e., Arctic, north Pacific, south Pacific, north Atlantic, south Atlantic, Indian, and Southern), we identified the surface pixels within their boundary. Then, we conducted four Kruskall–Wallis H tests (one per metric) to examine potential differences in the distribution of metric values among the oceans.

Connectivity between marine areas. To identify the location of the future analogs of broader marine areas, we partitioned the ocean realm based on the Major Fishing Areas (MFAs) of the Food and Agriculture Organization (FAO) categorization. We used graph theory[63,64] to describe the properties of the climate connectivity among the MFA network. A graph consists of a set of nodes (here the MFAs), with links between them depicting the strength of their connection[63,64]. This graph is directed, which means that considering two areas, namely A and B, the link from A to B is not necessarily equal to the link from B to A, depending on which area is considered as the present climate and which one is considered as its future analog. Since future analogs of local climate conditions could also be identified within the same MFA, links from an area towards itself were also included. To evaluate the links between each pair of MFAs, we quantified (i) the percentage of pixels in the first MFA that have a future analog in the second MFA and (ii) the percentage of pixels in the second MFA that will host analogs of the first MFA. Finally, we accounted for the mean percentage of pixels with analogs, as well as the mean percentage of pixels that will host analogs per MFA.

Thermal analogs of biodiversity hotspots. We considered six distinct marine biodiversity hotspots, as delineated by Ramirez et al.[20], based on the distributions of 2183 marine species (fish, marine mammals, and seabirds). We interpolated the biodiversity hotspots data from the initial grid of $0.5° \times 0.5°$ resolution to a grid of $1° \times 1°$ resolution, using the "resample" function in R, under nearest neighbor interpolation. We identified the thermal analogs of the pixels of each of the six hotspots, while in case of multiple analogs per pixel, we maintained the one having the trajectory that minimizes the exposure to dissimilar climates.

Data availability

Data on sea surface temperature models from CMIP6 was extracted from Earth System Grid Federation (ESGF) node in Deutsches Klimarechenzentrum (DKRZ). Ocean boundaries were extracted from the International Hydrographic Organization (IHO) Sea Areas v3 (www.marineregions.com). Major Fishing Areas (MFAs) were extracted from the Food and Agriculture Organization (FAO) (www.marineregions.com). Data on biodiversity hotspots were extracted from the Spanish National Research Council [Consejo Superior de Investigaciones Científicas (CSIC)] digital repository. Source data for figures presented in this manuscript are available in Figshare:

Figures 1–3: https://doi.org/10.6084/m9.figshare.20747605.v2
Figure 4: https://doi.org/10.6084/m9.figshare.20747653.v2
Figure 5: https://doi.org/10.6084/m9.figshare.20748151.v2.

Code availability

Code used to calculate the metrics is available in Figshare: https://doi.org/10.6084/m9.figshare.20748301.v3.

Received: 28 May 2022; Accepted: 26 September 2022;
Published online: 14 October 2022

References

1. Sydeman, W. J., Poloczanska, E., Reed, T. E. & Thompson, S. A. Climate change and marine vertebrates. *Science (1979)* **350**, 772–777 (2015).
2. Lind, S., Ingvaldsen, R. B. & Furevik, T. Arctic warming hotspot in the northern Barents Sea linked to declining sea-ice import. *Nat. Clim. Chang.* **8**, 634–639 (2018).
3. Pinsky, M. L., Selden, R. L. & Kitchel, Z. J. Climate-driven shifts in marine species ranges: scaling from organisms to communities. *Ann. Rev. Mar. Sci.* **12**, 153–179 (2020).
4. Cheng, L., Abraham, J., Hausfather, Z. & Trenberth, K. E. How fast are the oceans warming? *Science (1979)* **363**, 128–129 (2019).
5. Henson, S. A. et al. Rapid emergence of climate change in environmental drivers of marine ecosystems. *Nat Commun.* **8**, 1–9 (2017).
6. Babcock, R. C. et al. Severe continental-scale impacts of climate change are happening now: extreme climate events impact marine habitat forming communities along 45% of Australia's coast. *Front Mar Sci.* **6**, 411 (2019).
7. Smale, D. A. et al. Marine heatwaves threaten global biodiversity and the provision of ecosystem services. *Nat Clim Chang.* **9**, 306–312 (2019).
8. Perry, A. L., Low, P. J., Ellis, J. R. & Reynolds, J. D. Climate change and distribution shifts in marine fishes. *Science (1979)* **308**, 1912–1915 (2005).
9. Last, P. R. et al. Long-term shifts in abundance and distribution of a temperate fish fauna: a response to climate change and fishing practices. *Glob. Ecol. Biogeogr.* **20**, 58–72 (2011).
10. Sorte, C. J. B., Williams, S. L. & Carlton, J. T. Marine range shifts and species introductions: comparative spread rates and community impacts. *Glob. Ecol. Biogeogr.* **19**, 303–316 (2010).
11. Fossheim, M. et al. Recent warming leads to a rapid borealization of fish communities in the Arctic. *Nat. Clim. Chang.* **5**, 673–677 (2015).
12. Lenoir, J. et al. Species better track climate warming in the oceans than on land. *Nat. Ecol. Evol.* **4**, 1044–1059 (2020).
13. Nuñez, T. A. et al. Connectivity planning to address climate change. *Conserv. Biol.* **27**, 407–416 (2013).
14. Burrows, M. T. et al. Geographical limits to species-range shifts are suggested by climate velocity. *Nature* **507**, 492–495 (2014).
15. Hamann, A., Roberts, D. R., Barber, Q. E., Carroll, C. & Nielsen, S. E. Velocity of climate change algorithms for guiding conservation and management. *Glob. Chang. Biol.* **21**, 997–1004 (2015).
16. Dobrowski, S. Z. & Parks, S. A. Climate change velocity underestimates climate change exposure in mountainous regions. *Nat. Commun.* **7**, 1–8 (2016).
17. Carroll, C., Parks, S. A., Dobrowski, S. Z. & Roberts, D. R. Climatic, topographic, and anthropogenic factors determine connectivity between current and future climate analogs in North America. *Glob. Chang. Biol.* **24**, 5318–5331 (2018).
18. McRae, B. H., Dickson, B. G., Keitt, T. H. & Shah, V. B. Using circuit theory to model connectivity in ecology, evolution, and conservation. *Ecology* **89**, 2712–2724 (2008).
19. Adriaensen, F. et al. The application of 'least-cost'modelling as a functional landscape model. *Landsc Urban Plan* **64**, 233–247 (2003).
20. Ramírez, F., Afán, I., Davis, L. S. & Chiaradia, A. Climate impacts on global hot spots of marine biodiversity. *Sci. Adv.* **3**, e1601198 (2017).
21. Ruela, R., Sousa, M. C., deCastro, M. & Dias, J. M. Global and regional evolution of sea surface temperature under climate change. *Glob. Planet Change* **190**, 103190 (2020).
22. Tamarin-Brodsky, T., Hodges, K., Hoskins, B. J. & Shepherd, T. G. Changes in Northern Hemisphere temperature variability shaped by regional warming patterns. *Nat. Geosci.* **13**, 414–421 (2020).
23. Barlow, J. et al. The future of hyperdiverse tropical ecosystems. *Nature* **559**, 517–526 (2018).
24. Collins, M. et al. The impact of global warming on the tropical Pacific Ocean and El Niño. *Nat. Geosci.* **3**, 391–397 (2010).
25. Collin, R., Rebolledo, A. P., Smith, E. & Chan, K. Y. K. Thermal tolerance of early development predicts the realized thermal niche in marine ectotherms. *Funct. Ecol.* **35**, 1679–1692 (2021).
26. Nguyen, K. D. T. et al. Upper temperature limits of tropical marine ectotherms: global warming implications. *PLoS ONE* **6**, e29340 (2011).
27. Wernberg, T. et al. An extreme climatic event alters marine ecosystem structure in a global biodiversity hotspot. *Nat. Clim. Chang.* **3**, 78–82 (2013).
28. Chaudhary, C., Saeedi, H. & Costello, M. J. Bimodality of latitudinal gradients in marine species richness. *Trends Ecol. Evol.* **31**, 670–676 (2016).
29. Oremus, K. L. et al. Governance challenges for tropical nations losing fish species due to climate change. *Nat Sustain* **3**, 277–280 (2020).

30. Jones, M. C. & Cheung, W. W. L. Multi-model ensemble projections of climate change effects on global marine biodiversity. *ICES J. Mar. Sci.* **72**, 741–752 (2015).
31. Blowes, S. A. et al. The geography of biodiversity change in marine and terrestrial assemblages. *Science (1979)* **366**, 339–345 (2019).
32. Li, J. & Thompson, D. W. J. Widespread changes in surface temperature persistence under climate change. *Nature* **599**, 425–430 (2021).
33. Kornhuber, K. & Tamarin-Brodsky, T. Future changes in Northern Hemisphere summer weather persistence linked to projected Arctic warming. *Geophys. Res. Lett.* **48**, e2020GL091603 (2021).
34. Molinos, J. G. et al. Climate velocity and the future global redistribution of marine biodiversity. *Nat. Clim. Chang.* **6**, 83–88 (2016).
35. Burrows, M. T. et al. Ocean community warming responses explained by thermal affinities and temperature gradients. *Nat. Clim. Chang.* **9**, 959–963 (2019).
36. Pimiento, C. et al. Functional diversity of marine megafauna in the Anthropocene. *Sci. Adv.* **6**, eaay7650 (2020).
37. Albouy, C. et al. Global vulnerability of marine mammals to global warming. *Sci. Rep.* **10**, 1–12 (2020).
38. Constable, A. J. et al. Climate change and Southern Ocean ecosystems I: how changes in physical habitats directly affect marine biota. *Glob. Chang. Biol.* **20**, 3004–3025 (2014).
39. Rogers, A. D. et al. Antarctic futures: an assessment of climate-driven changes in ecosystem structure, function, and service provisioning in the Southern Ocean. *Ann. Rev. Mar. Sci.* **12**, 87–120 (2020).
40. Lester, S. E., Ruttenberg, B. I., Gaines, S. D. & Kinlan, B. P. The relationship between dispersal ability and geographic range size. *Ecol. Lett.* **10**, 745–758 (2007).
41. Grose, M. R. et al. Insights from CMIP6 for Australia's future climate. *Earths Future* **8**, e2019EF001469 (2020).
42. McKenna, S., Santoso, A., Gupta, A., sen, Taschetto, A. S. & Cai, W. Indian Ocean Dipole in CMIP5 and CMIP6: characteristics, biases, and links to ENSO. *Sci. Rep.* **10**, 1–13 (2020).
43. You, Q. et al. Temperature dataset of CMIP6 models over China: evaluation, trend and uncertainty. *Clim. Dyn.* **57**, 17–35 (2021).
44. Richter, I. & Tokinaga, H. An overview of the performance of CMIP6 models in the tropical Atlantic: mean state, variability, and remote impacts. *Clim. Dyn.* **55**, 2579–2601 (2020).
45. Cai, W. et al. Changing El Niño–Southern Oscillation in a warming climate. *Nat. Rev. Earth Environ.* **2**, 628–644 (2021).
46. Power, S. et al. Decadal climate variability in the tropical Pacific: characteristics, causes, predictability, and prospects. *Science (1979)* **374**, eaay9165 (2021).
47. Li, G. & Xie, S.-P. Tropical biases in CMIP5 multimodel ensemble: the excessive equatorial Pacific cold tongue and double ITCZ problems. *J. Clim.* **27**, 1765–1780 (2014).
48. Brito-Morales, I. et al. Climate velocity reveals increasing exposure of deep-ocean biodiversity to future warming. *Nat. Clim. Chang.* **10**, 576–581 (2020).
49. Robinson, L. M. et al. Pushing the limits in marine species distribution modelling: lessons from the land present challenges and opportunities. *Glob. Ecol. Biogeogr.* **20**, 789–802 (2011).
50. Chen, Y. et al. Estimating seasonal habitat suitability for migratory species in the Bohai Sea and Yellow Sea: a case study of Tanaka's snailfish (Liparis tanakae). *Acta Oceanologica Sinica* 1–9 (2022).
51. Almpanidou, V., Markantonatou, V. & Mazaris, A. D. Thermal heterogeneity along the migration corridors of sea turtles: implications for climate change ecology. *J Exp Mar Biol Ecol* **520**, 151223 (2019).
52. Plecha, S. M. & Soares, P. M. M. Global marine heatwave events using the new CMIP6 multi-model ensemble: from shortcomings in present climate to future projections. *Environ. Res. Lett.* **15**, 124058 (2020).
53. Brito-Morales, I. et al. Towards climate-smart, three-dimensional protected areas for biodiversity conservation in the high seas. *Nat. Clim. Chang.* 1–6 (2022).
54. Arafeh-Dalmau, N. et al. Incorporating climate velocity into the design of climate-smart networks of marine protected areas. *Methods Ecol. Evol.* **12**, 1969–1983 (2021).
55. McBride, M. M. et al. Antarctic krill Euphausia superba: spatial distribution, abundance, and management of fisheries in a changing climate. *Mar. Ecol. Prog. Ser.* **668**, 185–214 (2021).
56. Doxa, A., Kamarianakis, Y. & Mazaris, A. D. Spatial heterogeneity and temporal stability characterize future climatic refugia in Mediterranean Europe. *Glob. Chang Biol.* (2022).
57. Melo-Merino, S. M., Reyes-Bonilla, H. & Lira-Noriega, A. Ecological niche models and species distribution models in marine environments: a literature review and spatial analysis of evidence. *Ecol. Modell.* **415**, 108837 (2020).
58. Loarie, S. R. et al. The velocity of climate change. *Nature* **462**, 1052–1055 (2009).
59. García Molinos, J. et al. Improving the interpretability of climate landscape metrics: an ecological risk analysis of Japan's Marine Protected Areas. *Glob. Chang. Biol.* **23**, 4440–4452 (2017).
60. Sala, E. et al. Protecting the global ocean for biodiversity, food and climate. *Nature* **592**, 397–402 (2021).
61. Eyring, V. et al. Overview of the Coupled Model Intercomparison Project Phase 6 (CMIP6) experimental design and organization. *Geosci. Model Dev.* **9**, 1937–1958 (2016).
62. Riahi, K. et al. The shared socioeconomic pathways and their energy, land use, and greenhouse gas emissions implications: an overview. *Global Environ Change* **42**, 153–168 (2017).
63. Urban, D. & Keitt, T. Landscape connectivity: a graph-theoretic perspective. *Ecology* **82**, 1205–1218 (2001).
64. Petsas, P., Almpanidou, V. & Mazaris, A. D. Landscape connectivity analysis: new metrics that account for patch quality, neighbors' attributes and robust connections. *Landsc Ecol.* **36**, 3153–3168 (2021).

Acknowledgements

A.D., V.A., and A.D.M. were supported from the FutureMARES project that has received funding from the European Union's Horizon 2020 research and innovation programme under grant agreement No 869300. P.P. was supported by the Hellenic Foundation for Research and Innovation (HFRI) under the HFRI PhD Fellowship grand (Fellowship Number: 1018).

Author contributions

A.D.M. and P.P. conceived the ideas and designed the methodology. P.P. led the analysis and coding. V.A. and A.D. contributed to ecological knowledge and statistical analyses. All authors contributed critically to the drafts and gave final approval for publication.

Competing interests

The authors declare no competing interests.

Additional information

Supplementary information The online version contains supplementary material available at https://doi.org/10.1038/s43247-022-00569-5.

Correspondence and requests for materials should be addressed to Panagiotis Petsas.

Peer review information *Communications Earth & Environment* thanks Isaac Brito-Morales and the other, anonymous, reviewer(s) for their contribution to the peer review of this work. Primary Handling Editors: Clare Davis and Alienor Lavergne. Peer reviewer reports are available.

Reprints and permission information is available at http://www.nature.com/reprints

Publisher's note Springer Nature remains neutral with regard to jurisdictional claims in published maps and institutional affiliations.